ISSN 1063-7761, Journal of Experimental and Theoretical Physics, 2007, Vol. 105, No. 6, pp. 1107–1118. © Pleiades Publishing, Inc., 2007.

ATOMS, MOLECULES, OPTICS

Charged Higgs Boson in the Economical 3–3–1 Model[1]

D. V. Soa[a], D. L. Thuy[a], L. N. Thuc[a], and T. T. Huong[b]

[a] *Department of Physics, Hanoi University of Education, Hanoi, Vietnam*

[b] *Institute of Physics, VAST, Hanoi 10000, Vietnam*

e-mail: dvsoa@assoc.iop.vast.ac.vn

Received March 14, 2007

Abstract—The $SU(3)_C \otimes SU(3)_L \otimes U(1)_X$ gauge model with two Higgs triplets (the economical 3–3–1 model) is presented. The minimal Higgs potential is considered in detail, and new Higgs bosons with the mass proportional to the bilepton mass are predicted. In the effective approximation, the charged Higgs bosons $H_2^{\pm}$ are scalar bileptons, while the neutral scalar bosons H^0 and H_1^0 do not carry a lepton number. The couplings of the charged Higgs bosons to leptons and quarks are given. We show that Yukawa couplings of $H_2^{\pm}$ to ordinary leptons and quarks are lepton-number violating. The pair production of $H_2^{\pm}$ at high-energy e^+e^- colliders with the polarization of the e^+, e^- beams is studied in detail. A numerical evaluation shows that, if the Higgs mass is not too heavy, then the reaction can give an observable cross section in future colliders at a high degree of polarization. The reaction $e^+e^- \longrightarrow H_2^{\pm}W^{\mp}$ is also examined. We show that the production cross sections of $H_2^{\pm}W^{\mp}$ are very small, much below the pair production of $H_2^{\pm}$, and, therefore, the associated production of $H_2^{\pm}$ and $W^{\mp}$ is, in general, not expected to lead to easily observable signals in the e^+e^- annihilation.

PACS numbers: 12.60.Fr, 14.80.Cp, 12.60.Cn, 14.80.Mz

DOI: 10.1134/S1063776107120023

1. INTRODUCTION

Recent neutrino experimental results [1] established the fact that neutrinos have masses and the standard model (SM) must be extended. Among the extensions beyond the SM, the models based on the $SU(3)_C \otimes SU(3)_L \otimes U(1)_X$ (3–3–1) gauge group have some intriguing features. First, they can provide a partial explanation of the generation number problem. Second, the third-quark generation has to be different from the first two, which leads to a possible explanation of why the top quark is uncharacteristically heavy.

There are two main versions of the 3–3–1 models. In one of them [2], the three known left-handed lepton components for each generation are associated with three $SU(3)_L$ triplets as $(\nu_l, l, l^c)_L$, where l_L^c is related to the right-handed isospin singlet of the charged lepton l in the SM. The scalar sector of this model is quite complicated (three triplets and one sextet). In the second version [3], three $SU(3)_L$ lepton triplets are of the form $(\nu_l, l, \nu_l^c)_L$, where ν_l^c is related to the right-handed component of the neutrino field ν_l (a model with right-handed neutrinos). The scalar sector of this model requires three Higgs triplets, and we, therefore, call this version the 3–3–1 model with three Higgs triplets (331RH3HT) in what follows. It is interesting to note that, in the 331RH3HT, two Higgs triplets have the same $U(1)_X$ charge with two neutral components at their top and bottom. Allowing these neutral components to have vacuum expectation values (VEVs), we can reduce the number of Higgs triplets to two. Based on these results, a model with two Higgs triplets, the economical 3–3–1 model, was recently proposed [4]. This model contains a very important advantage: there is no new parameter, but its Higgs sector is very simple, and, hence, a significant number of free parameters are reduced. In the Higgs sector of this model, there are four physical Higgs bosons. Two of them are neutral physical fields (H^0 and H_1^0), and the others are singly charged bosons $H_2^{\pm}$.

The Higgs boson plays an important role in the SM, being responsible for the generation of the masses of all elementary particles (leptons, quarks, and gauge bosons). The experimental detection of them will be a great triumph of the electroweak interactions and will mark a new stage in high-energy physics. However, the mass of the Higgs boson is a free parameter.[2] The trilinear Higgs self-coupling can be measured directly in the pair production of the Higgs particle at hadron and

[1] The text was submitted by the authors in English.

[2] For a review on the Higgs sector in the SM, see [5].

high-energy e^+e^- linear colliders [6–9] or at photon colliders [10]. Interactions among the SM gauge bosons and Higgs bosons in the economical 3–3–1 model were studied in detail in our earlier work [11]. The trilinear gauge boson couplings in the 3–3–1 models were presented in [12]. Production of bileptons in high-energy collisions [13] and the single Z' production at CLIC based on e–γ collisions were studied in [14]. The discovery potential for doubly charged Higgs bosons and the possibility of detecting neutral Higgs boson in the minimal version at e^+e^- colliders was considered in [15, 16]. The production of the Higgs bosons in the 331RH3HT at the CERN LHC was studied in [17]. The distinguishing little-Higgs production and simple group models at the LHC and ILC were also recently discussed [18].

The polarization of electron and positron beams gives a very effective means to control the effect of the SM processes on the experimental analyses. Beam polarization is also an indispensable tool in identifying and studying new particles and their interactions. In this paper, we consider some properties of $H_2^{\pm}$ in the 3–3–1 economical model and future experiments on the production of singly charged Higgs boson in high-energy collisions with the polarization of e^+, e^- beams.

This paper is organized as follows. In Section 2, we give a brief review of the economical 3–3–1 model. Section 3 presents the minimal Higgs potential in detail. In Section 4, we consider the coupling of the charged Higgs boson with leptons and quarks. Section 5 represents a detailed calculation of the cross section of the $H_2^{\pm}$ pair production with the polarization of e^+, e^- beams. The associated production of $H_2^{\pm}$ and $W^{\mp}$ via neutral bosons Z and Z' is given in Section 6. We summarize our results and make conclusions in Section 7.

2. A REVIEW OF THE ECONOMICAL 3–3–1 MODEL

The particle content in this model, which is anomaly free, is given by [4]

$$\psi_{aL} = (\nu_{aL}, l_{aL}, N_{aL})^T \sim \left(1, 3, -\frac{1}{3}\right), \quad l_{aR} \sim (1, 1, -1), \tag{1}$$

where $a = 1, 2, 3$ is a family index. The right-handed neutrino is denoted by $N_L \equiv (\nu_R)^c$ and

$$\begin{gathered} Q_{1L} = (u_1, d_1, U)_L^T \sim \left(3, \frac{1}{3}\right), \\ Q_{\alpha L} = (d_\alpha, -u_\alpha, D_\alpha)_L^T \sim (3^*, 0), \quad \alpha = 2, 3, \\ u_{aR} \sim \left(1, \frac{2}{3}\right), \quad d_{aR} \sim \left(1, -\frac{1}{3}\right), \\ U_R \sim \left(1, \frac{2}{3}\right), \quad D_{\alpha R} \sim \left(1, -\frac{1}{3}\right). \end{gathered} \tag{2}$$

Electric charges of exotic quarks U and D_α are the same as for usual quarks, i.e., $q_U = 2/3$ and $q_{D_\alpha} = -1/3$. The $SU(3)_L \otimes U(1)_X$ gauge group is broken spontaneously in two steps. In the first step, it is embedded in the SM group via a Higgs scalar triplet

$$\chi = (\chi_1^0, \chi_2^-, \chi_3^0)^T \sim \left(3, -\frac{1}{3}\right), \tag{3}$$

endowed with the VEV

$$\langle\chi\rangle = \frac{1}{\sqrt{2}}(u, 0, \omega)^T. \tag{4}$$

In the second step, to embed the gauge group of the SM in $U(1)_Q$, another Higgs scalar triplet

$$\phi = (\phi_1^+, \phi_2^0, \phi_3^+)^T \sim \left(3, \frac{2}{3}\right) \tag{5}$$

is needed with the VEV

$$\langle\phi\rangle = \frac{1}{\sqrt{2}}(0, v, 0)^T. \tag{6}$$

The Yukawa interactions that induce the fermion masses can be written in the most general form as

$$\mathcal{L}_Y = (\mathcal{L}_Y^\chi + \mathcal{L}_Y^\phi) + \mathcal{L}_Y^{\text{mix}}, \tag{7}$$

where

$$\begin{aligned} (\mathcal{L}_Y^\chi + \mathcal{L}_Y^\phi) &= h'_{11}\bar{Q}_{1L}\chi U_R + h'_{\alpha\beta}\bar{Q}_{\alpha L}\chi^* D_{\beta R} \\ &+ h_{ij}^e \bar{\psi}_{iL}\phi e_{jR} + h_{ij}^\epsilon \epsilon_{pmn}(\bar{\psi}_{iL}^c)_p(\psi_{jL})_m(\phi)_n \\ &+ h_{1i}^d \bar{Q}_{1L}\phi d_{iR} + h_{\alpha i}^d \bar{Q}_{\alpha L}\phi^* u_{iR} + \text{H.c.}, \end{aligned} \tag{8}$$

$$\begin{aligned} \mathcal{L}_Y^{\text{mix}} &= h_{1i}^u \bar{Q}_{1L}\chi u_{iR} + h_{\alpha i}^u \bar{Q}_{\alpha L}\chi^* d_{iR} \\ &+ h''_{1\alpha}\bar{Q}_{1L}\phi D_{\alpha R} + h''_{\alpha 1}\bar{Q}_{\alpha L}\phi^* U_R + \text{H.c.} \end{aligned} \tag{9}$$

The VEV ω gives mass to the exotic quarks U and D_α and the new gauge bosons Z', X, and Y, while the VEVs u and v give mass to the quarks u_a and d_a, the leptons l_a, and the ordinary gauge bosons Z and W. To preserve the correspondence with the effective theory, the VEVs in this model must satisfy the constraint

$$u^2 \ll v^2 \ll \omega^2. \tag{10}$$

The masses of the gauge bosons are

$$M_W^2 = \frac{g^2 v^2}{4}, \tag{11}$$

$$M_Y^2 = \frac{g^2}{4}(u^2 + v^2 + \omega^2), \tag{12}$$

$$M_X^2 = \frac{g^2}{4}(\omega^2 + u^2), \tag{13}$$

and

$$M_{Z^1}^2 \approx \frac{g^2}{4c_W^2}(v^2 - 3u^2), \quad (14)$$

$$M_{Z^2}^2 \approx \frac{g^2 c_W^2 \omega^2}{3 - 4s_W^2}. \quad (15)$$

Relations (11), (12), and (13) imply the splitting between the bilepton masses similar to the law of Pythagoras

$$M_Y^2 = M_X^2 + M_W^2. \quad (16)$$

Therefore, the charged bilepton Y is slightly heavier than the neutral one X. We recall that a similar relation in the 331RH3HT is $|M_Y^2 - M_X^2| \le m_W^2$ [3].

3. HIGGS POTENTIAL

In this model, the most general Higgs potential has the very simple form

$$\begin{aligned} V(\chi, \phi) &= \mu_1^2\chi^\dagger\chi + \mu_2^2\phi^\dagger\phi + \lambda_1(\chi^\dagger\chi)^2 + \lambda_2(\phi^\dagger\phi)^2 \\ &+ \lambda_3(\chi^\dagger\chi)(\phi^\dagger\phi) + \lambda_4(\chi^\dagger\phi)(\phi^\dagger\chi). \end{aligned} \quad (17)$$

We note that there is no trilinear scalar coupling, which makes the Higgs potential much simpler than that in the 331RH3HT [19] and closer to that of the SM. The analysis in [20] shows that, after symmetry breaking, there are eight Goldstone bosons and four physical scalar fields. One of two physical neutral scalars is the SM Higgs boson.

We shift the Higgs fields into physical ones,

$$\chi = \begin{pmatrix} x_1^0 + \frac{u}{\sqrt{2}} \\ \chi_2^- \\ \chi_3^0 + \frac{\omega}{\sqrt{2}} \end{pmatrix}, \quad \phi = \begin{pmatrix} \phi_1^+ \\ \phi_2^0 + \frac{v}{\sqrt{2}} \\ \phi_3^+ \end{pmatrix}. \quad (18)$$

With (18) substituted into (17), the potential becomes

$$\begin{aligned} V(\chi, \phi) &= \mu_1^2\Big[\Big(\chi_1^{0*} + \frac{u}{\sqrt{2}}\Big)\Big(\chi_1^0 + \frac{u}{\sqrt{2}}\Big) \\ &+ \chi_2^+\chi_2^- + \Big(\chi_3^{0*} + \frac{\omega}{\sqrt{2}}\Big)\Big(\chi_3^0 + \frac{\omega}{\sqrt{2}}\Big)\Big] \\ &+ \mu_2^2\Big[\phi_1^-\phi_1^+ + \Big(\phi_2^{0*} + \frac{v}{\sqrt{2}}\Big)\Big(\phi_2^0 + \frac{v}{\sqrt{2}}\Big) + \phi_3^-\phi_3^+\Big] \\ &+ \lambda_1\Big[\Big(\chi_1^{0*} + \frac{u}{\sqrt{2}}\Big)\Big(\chi_1^0 + \frac{u}{\sqrt{2}}\Big) \\ &+ \chi_2^+\chi_2^- + \Big(\chi_3^{0*} + \frac{\omega}{\sqrt{2}}\Big)\Big(\chi_3^0 + \frac{\omega}{\sqrt{2}}\Big)\Big]^2 \\ &+ \lambda_2\Big[\phi_1^-\phi_1^+ + \Big(\phi_2^{0*} + \frac{v}{\sqrt{2}}\Big)\Big(\phi_2^0 + \frac{v}{\sqrt{2}}\Big) + \phi_3^-\phi_3^+\Big]^2 \\ &+ \lambda_3\Big[\Big(\chi_1^{0*} + \frac{u}{\sqrt{2}}\Big)\Big(\chi_1^0 + \frac{u}{\sqrt{2}}\Big) \\ &+ \chi_2^+\chi_2^- + \Big(\chi_3^{0*} + \frac{\omega}{\sqrt{2}}\Big)\Big(\chi_3^0 + \frac{\omega}{\sqrt{2}}\Big)\Big] \\ &\times\Big[\phi_1^-\phi_1^+ + \Big(\phi_2^{0*} + \frac{v}{\sqrt{2}}\Big)\Big(\phi_2^0 + \frac{v}{\sqrt{2}}\Big) + \phi_3^-\phi_3^+\Big] \\ &+ \lambda_4\Big[\Big(\chi_1^{0*} + \frac{u}{\sqrt{2}}\Big)\phi_1^+ + \chi_2^+\Big(\phi_2^0 + \frac{v}{\sqrt{2}}\Big) \\ &+ \Big(\chi_3^{0*} + \frac{\omega}{\sqrt{2}}\Big)\phi_3^+\Big] \\ &\times\Big[\phi_1^-\Big(\chi_1^0 + \frac{u}{\sqrt{2}}\Big) + \Big(\phi_2^{0*} + \frac{v}{\sqrt{2}}\Big)\chi_2^- \\ &+ \phi_3^-\Big(\chi_3^0 + \frac{\omega}{\sqrt{2}}\Big)\Big]. \end{aligned} \quad (19)$$

From the above expression, we obtain constraint equations at the tree level

$$\mu_1^2 + \lambda_1(u^2 + \omega^2) + \lambda_3\frac{v^2}{2} = 0, \quad (20)$$

$$\mu_2^2 + \lambda_2 v^2 + \lambda_3\frac{(u^2 + \omega^2)}{2} = 0, \quad (21)$$

which imply that the Higgs vacua are not $SU(3)_L \otimes U(1)_X$ singlets. As a result, the gauge symmetry is broken spontaneously. The nonzero values of χ and ϕ at the minimum value of $V(\chi, \phi)$ can be easily obtained as

$$\begin{aligned} \chi^+\chi &= \frac{u^2 + \omega^2}{2} = \frac{\lambda_3\mu_2^2 - 2\lambda_2\mu_1^2}{4\lambda_1\lambda_2 - \lambda_3^2}, \\ \phi^+\phi &= \frac{v^2}{2} = \frac{\lambda_3\mu_1^2 - 2\lambda_1\mu_2^2}{4\lambda_1\lambda_2 - \lambda_3^2}. \end{aligned} \quad (22)$$

It is worth noting that any other choice of u and ω for the vacuum value of χ satisfying (22) gives the same physics because it is related to (4) by an $SU(3)_L \otimes U(1)_X$ transformation. Thus, in general, we assume that $u \neq 0$.

Because u is the lepton-number violation parameter, the terms linear in u violate the lepton number. Applying constraint equations (20) and (21), we obtain the minimum value, mass terms, lepton-number conserving, and lepton-number violating interactions:

$$V(\chi, \phi) = V_{\min} + V^N_{\text{mass}} + V^C_{\text{mass}} + V_{LNC} + V_{LNV}, \quad (23)$$

where

$$V_{\min} = -\frac{\lambda_2}{4}v^4 - \frac{1}{4}(u^2+\omega^2)[\lambda_1(u^2+\omega^2)+\lambda_3 v^2],$$

$$V^N_{\text{mass}} = \lambda_1(uS_1+\omega S_3)^2 + \lambda_2 v^2 S_2^2 + \lambda_3 v(uS_1+\omega S_3)S_2, \quad (24)$$

$$V^C_{\text{mass}} = \frac{\lambda_4}{2}(u\phi_1^+ + v\chi_2^+ + \omega\phi_3^+) \times (u\phi_1^- + v\chi_2^- + \omega\phi_3^-), \quad (25)$$

$$\begin{aligned} V_{LNC} = {} & \lambda_1(\chi^+\chi)^2 + \lambda_2(\phi^+\phi)^2 \\ & + \lambda_3(\chi^+\chi)(\phi^+\phi) + \lambda_4(\chi^+\phi)(\phi^+\chi) \\ & + 2\lambda_1\omega S_3(\chi^+\chi) + 2\lambda_2 v S_2(\phi^+\phi) + \lambda_3 v S_2(\chi^+\chi) \\ & + \lambda_3\omega S_3(\phi^+\phi) + \frac{\lambda_4}{\sqrt{2}}(v\chi_2^- + \omega\phi_3^-)(\chi^+\phi) \\ & + \frac{\lambda_4}{\sqrt{2}}(v\chi_2^+ + \omega\phi_3^+)(\phi^+\chi), \end{aligned} \quad (26)$$

$$V_{LNV} = 2\lambda_1 uS_1(\chi^+\chi) + \lambda_3 uS_1(\phi^+\phi) + \frac{\lambda_4}{\sqrt{2}}u[\phi_1^-(\chi^+\phi) + \phi_1^+(\phi^+\chi)]. \quad (27)$$

We here expanded the neutral Higgs fields as

$$\chi_1^0 = \frac{S_1 + iA_1}{\sqrt{2}}, \quad \chi_3^0 = \frac{S_3 + iA_3}{\sqrt{2}}, \quad \phi_2^0 + \frac{S_2 + iA_2}{\sqrt{2}}. \quad (28)$$

In the literature, the real parts (S_i, i = 1, 2, 3) are also called CP-even scalars and the imaginary parts (A_i, i = 1, 2, 3) are called CP-odd scalars. In this paper, we call them scalar and pseudoscalar fields, respectively. As expected, the lepton-number violating part V_{LNC} is linear in u and trilinear in the scalar fields.

In the pseudoscalar sector, all fields are Goldstone bosons: $G_1 = A_1$, $G_2 = A_2$, and $G_3 = A_3$ (see Eq. (24)). The scalar fields S_1, S_2, and S_3 acquire masses via (24), and we, therefore, obtain one Goldstone boson G_4 and two neutral physical fields: the SM H^0 and the new H_1^0 with the masses

$$\begin{aligned} m^2_{H^0} = {} & \lambda_2 v^2 + \lambda_1(u^2+\omega^2) \\ & - \sqrt{[\lambda_2 v^2 - \lambda_1(u^2+\omega^2)]^2 + \lambda_3^2 v^2(u^3+\omega^2)} \\ & \approx \frac{4\lambda_1\lambda_2 - \lambda_3^2}{2\lambda_1}v^2, \end{aligned} \quad (29)$$

$$\begin{aligned} M^2_{H_1^0} = {} & \lambda_2 v^2 + \lambda_1(u^2+\omega^2) \\ & + \sqrt{[\lambda_2 v^2 - \lambda_1(u^2+\omega^2)]^2 + \lambda_3^2 v^2(u^2+\omega^2)} \approx 2\lambda_1\omega^2. \end{aligned} \quad (30)$$

In terms of the scalars, the Goldstone and Higgs fields are given by

$$G_4 = \frac{1}{\sqrt{1+t_\theta^2}}(S_1 - t_\theta S_3), \quad (31)$$

$$H^0 = c_\zeta S_2 - \frac{s_\zeta}{\sqrt{1+t_\theta^2}}(t_\theta S_1 + S_3), \quad (32)$$

$$H_1^0 = s_\zeta S_2 + \frac{c_\zeta}{\sqrt{1+t_\theta^2}}(t_\theta S_1 + S_3), \quad (33)$$

where

$$t_{2\zeta} \equiv \frac{\lambda_3 M_W M_X}{\lambda_1 M_X^2 - \lambda_2 M_W^2}. \quad (34)$$

It follows from Eq. (30) that the mass of the new Higgs boson $M_{H_1^0}$ is related to the mass of the bilepton gauge X^0 (or $Y^\pm$ via the law of Pythagoras) through

$$\begin{aligned} M^2_{H_1^0} = {} & \frac{8\lambda_1}{g^2}M_X^2\left[1 + O\left(\frac{M_W^2}{M_X^2}\right)\right] \\ = {} & \frac{2\lambda_1 s_W^2}{\pi\alpha}M_X^2\left[1 + O\left(\frac{M_W^2}{M_X^2}\right)\right] \approx 18.8\lambda_1 M_X^2. \end{aligned} \quad (35)$$

Here, we use $\alpha = 1/128$ and $s_W^2 = 0.231$.

In the charged Higgs sector, the mass terms for (ϕ_1, χ_2, ϕ_3) are given by (25), and, hence, there are two Goldstone bosons and one physical scalar field:

$$H_2^+ \equiv \frac{1}{\sqrt{u^2+v^2+\omega^2}}(u\phi_1^+ + v\chi_2^+ + \omega\phi_3^+) \quad (36)$$

with the mass

$$\begin{aligned} M^2_{H_2^+} = {} & \frac{\lambda_4}{2}(u^2+v^2+\omega^2) = 2\lambda_4\frac{M_Y^2}{g^2} \\ = {} & \frac{s_W^2\lambda_4}{2\pi\alpha}M_Y^2 \approx 4.7\lambda_4 M_Y^2. \end{aligned} \quad (37)$$

The remaining two Goldstone bosons are

$$G_5^+ = \frac{1}{\sqrt{1+t_\theta^2}}(\phi_1^+ - t_\theta\phi_3^+), \tag{38}$$

$$G_6^+ = \frac{1}{\sqrt{(1+t_\theta^2)(u^2+v^2+\omega^2)}} \times [v(t_\theta\phi_1^+ + \phi_3^+) - \omega(1+t_\theta^2)\chi_2^+]. \tag{39}$$

Thus, all pseudoscalars are eigenstates and are massless (Goldstone). The other physical fields are related to the scalars in the weak basis by the linear transformations

$$\begin{pmatrix} H^0 \\ H_1^0 \\ G_4 \end{pmatrix} = \begin{pmatrix} -s_\zeta s_\theta & c_\zeta & -s_\zeta c_\theta \\ c_\zeta s_\theta & s_\zeta & c_\zeta c_\theta \\ c_\theta & 0 & -s_\theta \end{pmatrix} \begin{pmatrix} S_1 \\ S_2 \\ S_3 \end{pmatrix}, \tag{40}$$

$$\begin{pmatrix} H_2^+ \\ G_5^+ \\ G_6^+ \end{pmatrix} = \frac{1}{\sqrt{\omega^2+c_\theta^2 v^2}} \times \begin{pmatrix} \omega s_0 & v c_\theta & \omega c_\theta \\ c_\theta\sqrt{\omega^2+c_\theta^2 v^2} & 0 & -s_\theta\sqrt{\omega^2+c_\theta^2 v^2} \\ \frac{v s_{2\theta}}{2} & -\omega & v c_\theta^2 \end{pmatrix} \begin{pmatrix} \phi_1^+ \\ \chi_2^+ \\ \phi_3^+ \end{pmatrix}. \tag{41}$$

From (29) and (30), we reproduce the result in [20]:

$$\lambda_1 > 0, \quad \lambda_2 > 0, \quad 4\lambda_1\lambda_2 > \lambda_3^2. \tag{42}$$

Equation (37) shows that the mass of the massive charged Higgs boson $H_2^\pm$ is proportional to the mass of the charged bilepton Y through the Higgs self-coupling constant $\lambda_4 > 0$. The same is true for the SM Higgs boson H^0 ($M_{H^0} \sim M_W$) and the new H_1^0 ($M_{H_1^0} \sim M_X$). Combining (42) with constraint equations (20) and (21), we obtain that $\lambda_3 < 0$.

To finish this section, we comment on our physical Higgs bosons. In the effective approximation $w^2 \gg v^2$, u^2, it follows from Eqs. (40) and (41) that

$$\begin{gathered} H^0 \sim S_2, \quad H_1^0 \sim S_3, \quad G_4 \sim S_1, \\ H_2^+ \sim \phi_3^+, \quad G_5^+ \sim \phi_1^+, \quad G_6^+ \sim \chi_2^+. \end{gathered} \tag{43}$$

This means that, in the effective approximation, the charged boson H_2^- is a scalar bilepton (with lepton number $L = 2$), and the neutral scalar bosons H^0 and H_1^0 do not carry a lepton number ($L = 0$).

4. INTERACTION OF $H_2^\pm$ WITH LEPTONS AND QUARKS

Substituting Eq. (41) into Eqs. (8) and (9), we obtain the couplings of $H_2^\pm$ to leptons and quarks as

$$L_Y^{\text{lepton}} = \frac{\omega H_2^+}{\sqrt{\omega^2+c_\theta^2 v^2}}[s_\theta(h_{ij}^e \bar{\nu}_{iL} e_{jR} - 2h_{ij}^\epsilon \bar{\nu}_{iL}^c e_{jL}) + c_\theta(h_{ij}^e \bar{\nu}_{iR}^c e_{jR} + 2h_{ij}^\epsilon \bar{\nu}_{iL}^c e_{jL})] + \text{H.c.} \tag{44}$$

and

$$\mathcal{L}_Y^{\chi(\text{quark})} = \frac{v c_\theta}{\sqrt{\omega^2+c_\theta^2 v^2}} \times [h'_{11} H_2^- \bar{d}_{1L} U_R - h'_{\alpha\beta} H_2^+ \bar{u}_{\alpha L} D_{\beta R}] + \text{H.c.}, \tag{45}$$

$$\mathcal{L}_Y^{\phi(\text{quark})} = \frac{\omega}{\sqrt{\omega^2+c_\theta^2 v^2}}[h_{1i}^d H_2^+(s_\theta \bar{u}_{1L} + c_\theta \bar{U}_L) d_{iR} + h_{\alpha i}^d H_2^-(s_\theta \bar{d}_{\alpha L} + c_\theta \bar{D}_{\alpha L}) u_{iR}] + \text{H.c.}, \tag{46}$$

$$\mathcal{L}_Y^{\chi(\text{mix})} = \frac{v c_\theta}{\sqrt{\omega^2+c_\theta^2 v^2}} \times [h_{1i}^u H_2^- \bar{d}_{1L} u_{iR} - h_{\alpha i}^u H_2^+ \bar{u}_{\alpha L} d_{iR}] + \text{H.c.}, \tag{47}$$

$$\mathcal{L}_Y^{\phi(\text{mix})} = \frac{\omega}{\sqrt{\omega^2+c_\theta^2 v^2}}[h''_{1\alpha} H_2^+(s_\theta \bar{u}_{1L} + c_\theta \bar{U}_L) D_{\alpha R} + h''_{1\alpha} H_2^-(s_\theta \bar{d}_{\alpha L} + c_\theta \bar{D}_{\alpha L}) D_R] + \text{H.c.} \tag{48}$$

From Eqs. (44) and (46), we see that the Yukawa coupling of $H_2^\pm$ to the ordinary leptons and quarks violates the lepton number, because $L(H_2^\pm) = \pm 2$. In this case, the coupling coefficients are proportional to s_θ, which means that the Yukawa couplings are very weak. Interactions among the SM gauge bosons and Higgs bosons were studied in detail in [11]. From these couplings, all scalar fields including the neutral scalar H^0 and the Goldstone bosons were identified and their couplings to the usual gauge bosons such as the photon, the charged bosons $W^\pm$, the neutral Z, and also Z' were recovered without any additional conditions. We note that the CP-odd part of the Goldstone boson associated with the neutral non-Hermitian bilepton gauge boson G_{X^0} decouples, while its CP-even counterpart is involved in mixing in the same way as in the gauge boson sector.

5. PAIR PRODUCTION OF $H_2^\pm$ IN e^+e^- COLLIDERS

High-energy e^+e^- colliders have been essential instruments to search for the fundamental constituents of matter and their interactions. The possibility of

Table 1. Trilinear couplings of the pair $H_2^{\pm}$ to the neutral gauge bosons in the SM

Vertex	$A^{\mu}H_2^-\overleftrightarrow{\partial}_{\mu}H_2^+$	$Z^{\mu}H_2^-\overleftrightarrow{\partial}_{\mu}H_2^+$
Coupling	ie	$-igS_Wt_W$

detecting the neutral Higgs boson in the minimal version at e^+e^- colliders was considered in [16] and the production of the SM-like neutral Higgs boson at CERN LHC was studied in [17]. This section is devoted to the pair production of $H_2^{\pm}$ at e^+e^- colliders with the center-of-mass energy chosen as $\sqrt{s} \le 1000$ GeV (CLIC) [15, 16]. The trilinear couplings of $H_2^{\pm}$ to the neutral gauge bosons in the SM are given in Table 1 [11].

From Table 1, we can see that the production of $H_2^{\pm}$ in e^+e^- colliders occurs through the neutral gauge bosons in the SM. We now consider the process in which the initial state contains an electron and a positron and the final state contains a pair of $H_2^{\pm}$:

$$e^-(p_1) + e^+(p_2) \longrightarrow H_2^+(k_1) + H_2^-(k_2). \tag{49}$$

Straightforward calculation yields the following differential cross section (DCS) in the center-of-mass frame with the polarized e^+e^- beams:

$$\begin{aligned}\frac{d\sigma_{(P_+,P_-)}}{d\cos\theta} = \frac{K^3_{H_2^+H_2^-}\pi\alpha^2}{4s^2}\Bigg[\frac{1}{s^2}(1-P_+P_-) \\ -\frac{g_z[v_e(1-P_+P_-)-a_e(P_--P_+)]}{2c_Ws_Ws(s-m_Z^2)} \\ +\frac{g_z^2[(v_e^2+a_e^2)(1-P_-P_+)-2v_ev_a(P_--P_+)]}{16c_W^2s_W^2(s-m_Z^2)^2}\Bigg] \\ \times(1-\cos^2\theta),\end{aligned} \tag{50}$$

where θ is the angle between $\mathbf{p}_1$ and $\mathbf{k}_1$,

$$g = \frac{e}{s_W}, \quad g_Z = \frac{2\omega^2s_W^2 - v^2(4c_W^2-1)}{2s_Wc_W(\omega^2+v^2)},$$

$$v_e = -1+4s_W^2, \quad a_e = -1,$$

$$K_{H_2^+H_2^-} = [(s-m_{H_2^+}^2-m_{H_2^-}^2)^2 - 4m_{H_2^+}^2m_{H_2^-}^2]^{1/2}, \tag{51}$$

and P_+ and P_- are the respective polarization coefficients of the e^+ and e^- beams. The total cross section is given by

$$\begin{aligned}\sigma_{(P_+,P_-)} = \frac{K^3_{H_2^+H_2^-}\pi\alpha^2}{3s^2}\Bigg[\frac{1}{s^2}(1-P_+P_-) \\ -\frac{g_z[v_e(1-P_+P_-)-a_e(P_--P_+)]}{2c_Ws_Ws(s-m_Z^2)} \\ +\frac{g_z^2[(v_e^2+a_e^2)(1-P_-P_+)-2v_ev_a(P_--P_+)]}{16c_W^2s_W^2(s-m_Z^2)^2}\Bigg],\end{aligned} \tag{52}$$

where we take $m_Z = 91.1882$ GeV, $v = 246$ GeV, and $\omega = 1$ TeV [4].

Based on Eqs. (44) and (46), we analyze the behavior of the cross section for some high energies of e^+e^- colliders. In Fig. 1, we plot the cross section $\sigma_{(P_+,P_-)}$ as a function of the polarized coefficients (P_+, P_-). The collision energy is taken to be $\sqrt{s} = 1$ TeV and the Higgs mass is chosen as $m_{H_2^{\pm}} = 200$ GeV. The figure shows that the cross section has the maximum value $\sigma_{(P_+,P_-)} = 6 \times 10^{-2}$ pb at $P_- = -1$ and $P_+ = 1$, while $\sigma_0 = 2.1 \times 10^{-2}$ pb at $P_- = P_+ = 0$. The DCS as a function of $\cos\theta$ is shown in Fig. 2 (curve *1* for $P_- = P_+ = 0$ and curve *2* for $P_- = -1$, $P_+ = 1$). We see from Fig. 2 that the DCS has a maximum value at $\cos\theta = 0$, similar to the process $e^+e^- \longrightarrow Zh$ in the SM (while the DCS of the reactions $e^+e^- \longrightarrow ZZ$, ZA has the minimal value at $\cos\theta = 0$) [9]. The results show that the cross section with highly polarized e^+, e^- beams is approximately

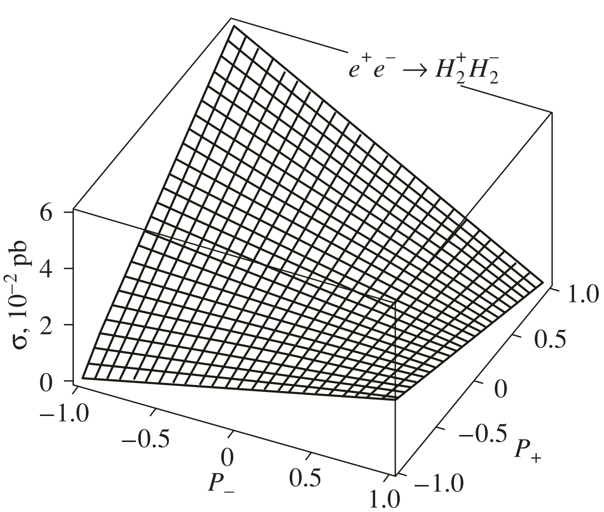

Fig. 1. The total cross section of the process $e^+e^- \longrightarrow H_2^{\pm}$ as a function of the polarization coefficients. The collision energy is taken to be $\sqrt{s} = 1$ TeV and the Higgs mass $m_{H_2^{\pm}} = 200$ GeV.

three times larger than those with unpolarized e^+, e^- beams. The dependence of the total cross section on the Higgs mass for fixed collision energies, typically $\sqrt{s}$ = 0.7, 0.85, 1 TeV, is also shown in Fig. 3 for $P_- = -1$, $P_+ = 1$ and in Fig. 4 for $P_- = P_+ = 0$. The Higgs mass is chosen as $200 \le m_H \le 500$ GeV. As we can see from the figures, at high energies, the cross section decreases as m_H increases. It is worth noting that there is no difference between two lines at $m_H \approx 240$, 260, and 300 GeV, with the respective cross sections given by $\sigma_{(P_+, P_-)}$ = 6×10^{-2}, 5×10^{-2}, and 4.2×10^{-2} pb. With the high integrated luminosity 500 fb^{-1} [8] and the Higgs mass chosen at a relatively low value of 200 GeV, the number of events with different values of $\sqrt{s}$ is given in Table 2. From these results, we can see that, with the high integrated luminosity and at the high degree of polarization of electron and positron beams, the production cross section may have observable values at moderately high energies. At the CLIC ($\sqrt{s}$ = 1 TeV), the number of events is approximately $N = 30500$, as expected.

6. ASSOCIATED PRODUCTION OF $H_2^{\pm}$ AND $W^{\mp}$ IN e^+e^- COLLIDERS

Similarly to Section 5, in this section, we evaluate the associated production of $H_2^{\pm}$ and $W^{\mp}$ at e^+e^- colliders via a $Z Z'$ exchange, which is lepton-number violating with $\Delta L = \pm 2$. The trilinear couplings of the pair $H_2^{\pm}W^{\mp}$ to the neutral gauge bosons in the economical 3–3–1 model are given in Table 3 [11]. Here, $U_{\alpha\beta}$ (α, β = 1, 2, 3, 4) is a mixing matrix of neutral gauge bosons given in the Appendix. The angle θ is the mixing angle between charged gauge bosons W and Y, which is defined by [4]

$$\tan\theta = u/\omega. \quad (53)$$

The decay of the charged gauge boson W into leptons and quarks analyzed in detail in [4] gives the upper limit $s_\theta \le 0.08$. We can see from Table 3 that the associated production of $H_2^{\pm}$ and $W^{\mp}$ at e^+e^- colliders occurs through the neutral gauge bosons Z and Z' in the s-channel

$$e^-(p_1) + e^+(p_2) \longrightarrow H_2^{\pm}(k_1) + W^{\mp}(k_2). \quad (54)$$

In this case, the DCS is given by

$$\begin{aligned}\frac{d\sigma_{(P_+, P_-)}}{d\cos\theta} = \frac{K_{H_2^{\pm}W^{\mp}}\pi^2\alpha^3}{2s^2}\Bigg\{&\frac{e_Z^2[(v_e^2 + a_e^2)(1 - P_-P_+) - 2v_e a_e(P_- - P_+)]}{16C_W^2S_W^2(s - m_Z^2)^2}\\ &+ \frac{e_Z'^2[(v_e'^2 + a_e'^2)(1 - P_-P_+) - 2v_e' a_e'(P_- - P_+)]}{16C_W^2S_W^2(s - m_{Z'}^2)^2}\\ &+ \frac{e_Z e_Z'[(v_e v_e' + a_e a_e')(1 - P_-P_+) - (v_e a_e' + v_e' a_e)(P_- - P_+)]}{8c_W^2s_W^2(s - m_Z^2)(s - m_{Z'}^2)}\Bigg\}\\ &\times\left\{-2s + \frac{K_{H_2^{\pm}W^{\mp}}^2}{2m_W^2}(1 - \cos^2\theta)\right\}\end{aligned} \quad (55)$$

and the total cross section is

$$\begin{aligned}\sigma_{(P_+, P_-)} = \frac{K_{H_2^{\pm}W^{\mp}}\pi^2\alpha^3}{2s^2}\Bigg\{&\frac{e_Z^2[(v_e^2 + a_e^2)(1 - P_-P_+) - 2v_e a_e(P_- - P_+)]}{16C_W^2S_W^2(s - m_Z^2)^2}\\ &+ \frac{e_Z'^2[(v_e'^2 + a_e'^2)(1 - P_-P_+) - 2v_e' a_e'(P_- - P_+)]}{16C_W^2S_W^2(s - m_{Z'}^2)^2}\\ &+ \frac{e_Z e_Z'[(v_e v_e' + a_e a_e')(1 - P_-P_+) - (v_e a_e' + v_e' a_e)(P_- - P_+)]}{8C_W^2S_W^2(s - m_Z^2)(s - m_{Z'}^2)}\Bigg\}\left\{-4s + \frac{2}{3}\frac{K_{H_2^{\pm}W^{\mp}}^2}{m_W^2}\right\},\end{aligned} \quad (56)$$

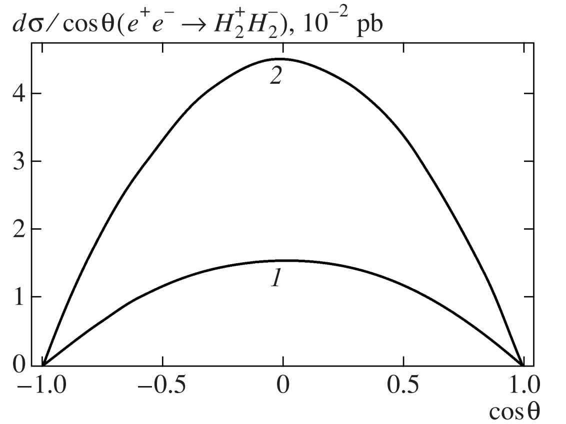

Fig. 2. The DCS of the process $e^+e^- \longrightarrow H_2^{\pm}$ as a function of $\cos\theta$. The collision energy is taken to be $\sqrt{s}$ = 1 TeV and the Higgs mass $m_{H_2^{\pm}}$ = 200 GeV. Curve *1* is for $P_- = 0$, $P_+ = 0$ and curve *2* is for $P_- = -1$, $P_+ = 1$.

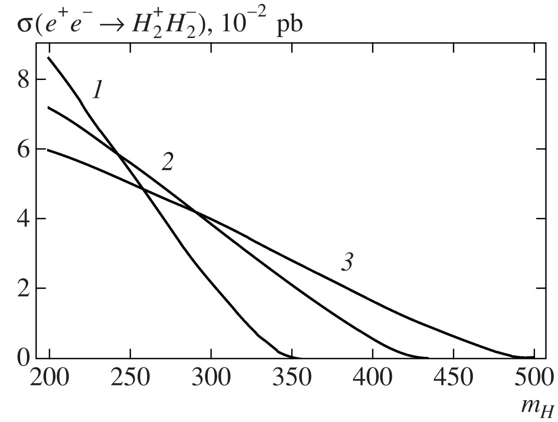

Fig. 3. The total cross section of the process $e^+e^- \longrightarrow H_2^{\pm}$ as a function of $m_{H_2^{\pm}}$ for $P_- = -1$ and $P_+ = 1$. The collision energies are chosen as $\sqrt{s}$ = 0.7 (*1*), 0.85 (*2*), and 1 (*3*) TeV.

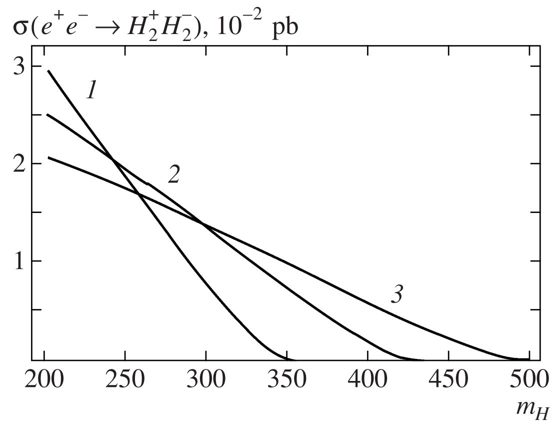

Fig. 4. The total cross section of the process $^+e^- \longrightarrow H_2^{\pm}$ as a function of $m_{H_2^{\pm}}$ for $P_- = P_+ = 0$. The collision energies are chosen as in Fig. 3.

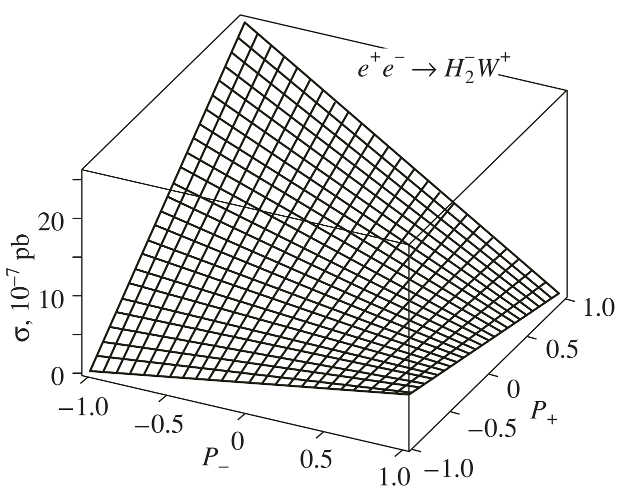

Fig. 5. The total cross section of the process $e^+e^- \longrightarrow H_2^- W^+$ as a function of the polarization coefficients. The collision energy is taken to be $\sqrt{s}$ = 1 TeV and the Higgs mass $m_{H_2^{\pm}}$ = 200 GeV.

where

$$v_e = -1 + 4S_W^2, \quad \alpha_e = -1, \quad v'_e = \frac{v_e}{\sqrt{4C_W^2 - 1}},$$

$$a'_e = \frac{a_e}{\sqrt{4C_W^2 - 1}},$$

$$e_Z = \frac{v\omega}{2S_W^2\sqrt{\omega^2 + c_\theta^2 v^2}} \times [s_\theta c_\theta(U_{12} + \sqrt{3}U_{22}) + c_{2\theta}U_{42}], \tag{57}$$

$$e'_Z = \frac{v\omega}{2S_W^2\sqrt{\omega^2 + c_\theta^2 v^2}} \times [s_\theta c_\theta(U_{13} + \sqrt{3}U_{23}) + c_{2\theta}U_{43}], \tag{58}$$

and

$$K_{H_2^{\pm}W^{\mp}} = [(s - m_{H_2^-}^2 - m_W^2)^2 - 4m_{H_2^-}^2 m_W^2]^{1/2}. \tag{59}$$

We here use data as in the previous section, with $m_{Z'}$ = 800 GeV [12]. For the convenience of the calculations, we take the upper value of the mixing angle $(s_\theta)_{\max}$ = 0.08.

Table 2. Number of events with the integrated luminosity 500 fb^{-1} and m_H = 200 GeV

$\sqrt{s}$, GeV	700	850	1000
$\sigma_{(P_+, P_-)}$, pb	8.7×10^{-2}	7.4×10^{-2}	6.1×10^{-2}
Number of events N	43500	37000	30500

We now evaluate the cross section in detail. In Fig. 5, we plot the total cross section $\sigma_{(P_+, P_-)}$ as a function of the polarized coefficients. The status is as in Fig. 1, the total cross section $\sigma_{(P_+, P_-)}$ takes the maximum value $\sigma_{(P_+, P_-)} = 2.5 \times 10^{-6}$ pb at $P_- = -1$ and $P_+ = 1$, while, if the e^+, e^- beams are not polarized, then $\sigma_0 = 0.8 \times 10^{-6}$ pb. In this case, the cross section is approximately 2.4×10^4 times smaller than those of the pair production $H_2^\pm$ under the same conditions. The DCS as a function of $\cos\theta$ at $\sqrt{s} = 1$ TeV is shown in Fig. 6 (curve *1* with $P_- = P_+ = 0$ and curve *2* with $P_- = -1$, $P_+ = 1$). We see that the behavior of the DCS is similar to that in Fig. 2. The Higgs mass dependence of the total cross section is shown in Fig. 7 for $P_- = -1$, $P_+ = 1$ and in Fig. 8 for $P_- = P_+ = 0$. The mass range is $200 \le m_H \le 800$ GeV, and the collision energies are chosen as above, $\sqrt{s} = 0.7$, 0.85, and 1 TeV, respectively. We can see from the figures that the total cross section decreases rapidly as m_H increases. Figure 7 shows that, at the lower bound of m_H, the respective cross sections are given by $\sigma_{(P_+, P_-)} = 17.5 \times 10^{-6}$, 4.8×10^{-6}, and 2.5×10^{-6} pb. We can see that Fig. 8 is the same as Fig. 7, but the cross sections are approximately three times smaller.

For comparison with the behavior at higher collision energies, we present the cross section as a function of m_H for the fixed energies $\sqrt{s} = 1$, 1.2, and 1.4 TeV in Fig. 9. It follows that, at higher values of $\sqrt{s}$, the total cross section decreases slowly, while at a lower energy ($\sqrt{s} = 1$ TeV), the total cross section decreases rapidly as m_H increases. This shows that the cross section of the pair $H_2^\pm W^\mp$ production is much smaller than that of the pair production of $H_2^\pm$ under the same conditions. We deduce that the associated production of $H_2^\pm$ and $W^\mp$ is, in general, not expected to lead to easily observable signals in e^+e^- collisions.

In the final state, $H_2^\pm$ can decay with modes as

$$\begin{aligned} H_2^\pm &\longrightarrow l^\pm \nu_l, \quad \tilde{U} d_a, \quad D_\alpha \tilde{u}_a, \\ &\searrow ZW^\pm, \quad Z'W^\pm, \quad XW^\pm, \quad ZY^\pm. \end{aligned} \tag{60}$$

We note that $H_2^\pm$ is a bilepton in the effective approximation. Assuming that the masses of the exotic quarks (U, D_α) are larger than $M_{H_2^\pm}$, we conclude that the hadron modes are absent in the decay of the charged Higgs boson. Because the Yukawa couplings of $H_2^\pm l^\mp \nu$ are very small, the main decay modes of $H_2^\pm$ are in the second line of (60). Because the exotic $H_2^\pm W^\mp Z'$ gauge bosons are heavy, the coupling of a singly charged Higgs boson with the weak gauge bosons, $H_2^\pm W^\mp Z$, may be dominating. The decay width is given by

$$\begin{aligned} \Gamma(H_2^\pm \longrightarrow W^\pm Z) &= \frac{\pi \alpha^2 e_Z^2 K_{H_2^\pm W^\mp}}{m_{H_2^\pm}^3} \\ &\times \left[2 + \frac{(m_{H_2^\pm}^2 - m_Z^2 - m_W^2)^2}{4 m_Z^2 m_W^2}\right]. \end{aligned} \tag{61}$$

Taking $200 \le m_{H_2^\pm} \le 800$ GeV, we have the decay width $2.1 \times 10^{-33} \le \Gamma(H_2^\pm \longrightarrow W^\pm Z) \le 3.4 \times 10^{-31}$ s^{-1}. It is interesting to note that the decay width of the main mode is also very small, because the considered process is lepton-number violating ($\Delta L = \pm 2$).

It is worth mentioning that the neutrinoless double-beta decay requires the violation of the lepton number. This can be useful in probing new physics beyond the SM [21]. Neutrino decay and neutrinoless double-beta decay in the 3–3–1 model were recently studied [22]. The results show that the relevance of the new contributions is determined by the mixing angle θ and the bilep-

Table 3. Trilinear couplings of the pair $H_2^\pm W^\mp$ to the neutral gauge bosons in the economical 3–3–1 model

Vertex	$ZH_2^\pm W^\mp$	$Z'H_2^\pm W^\mp$
Coupling	$\frac{g^2 v\omega}{2\sqrt{\omega^2 + c_\theta^2 v^2}}[s_\theta c_\theta(U_{12} + \sqrt{3}U_{22}) + c_{2\theta}U_{42}]$	$\frac{g^2 v\omega}{2\sqrt{\omega^2 + c_\theta^2 v^2}}[s_\theta c_\theta(U_{13} + \sqrt{3}U_{23}) + c_{2\theta}U_{43}]$

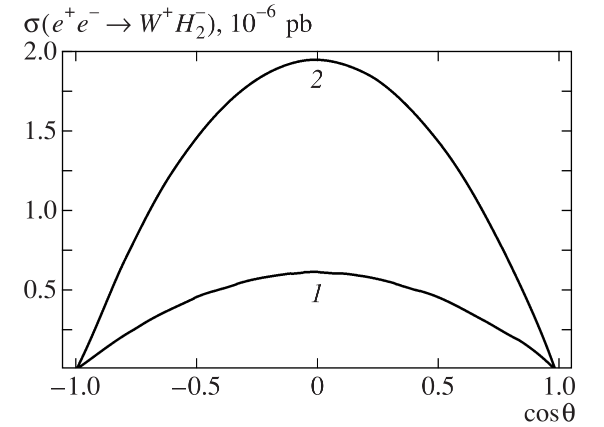

Fig. 6. The DCS of the process $e^+e^- \longrightarrow H_2^- W^+$ as a function of $\cos\theta$. The collision energy is taken to be $\sqrt{s} = 1$ TeV and the Higgs mass $m_{H_2^\pm} = 200$ GeV. Curve *1* is for $P_- = 0$, $P_+ = 0$ and curve *2* is for $P_- = -1$, $P_+ = 1$.

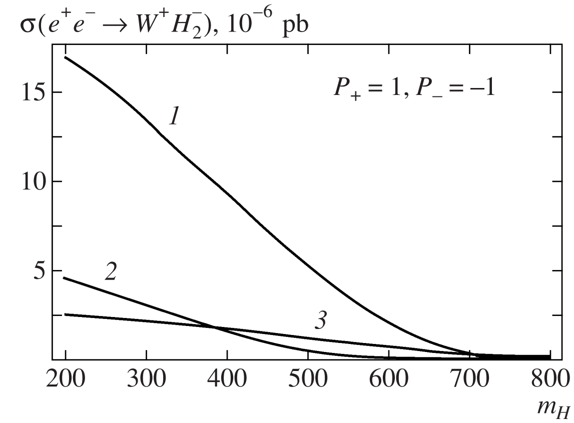

Fig. 7. The total cross section of the process $e^+e^- \longrightarrow H_2^\pm$ as a function of m_H for $P_- = -1$ and $P_+ = 1$. The collision energies are taken to be $\sqrt{s} = 0.7$ (*1*), 0.85 (*2*), and 1 (*3*) TeV.

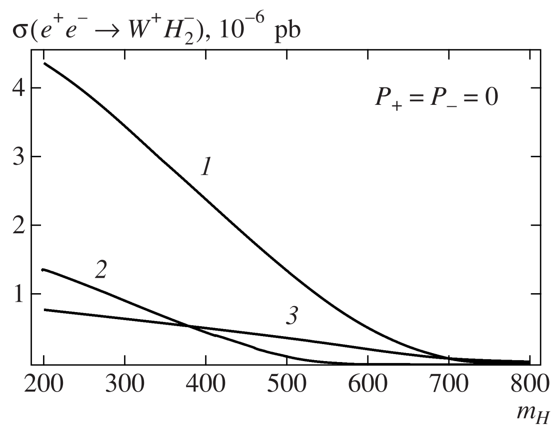

Fig. 8. The total cross section of the process $e^+e^- \longrightarrow H_2^- W^+$ as a function of m_H for $P_- = P_+ = 0$. The collision energies are chosen as in Fig. 7.

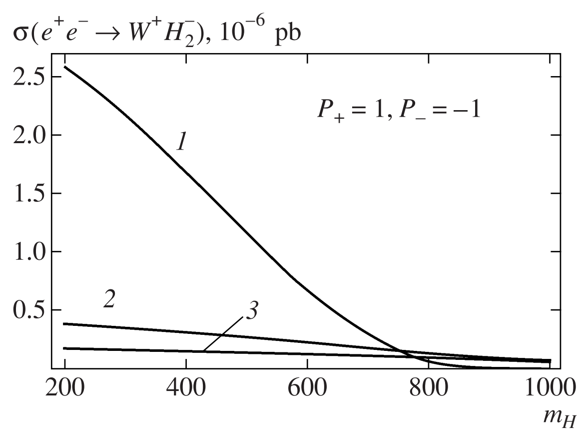

Fig. 9. Same as Fig. 7, but $\sqrt{s} = 1.0$ (*1*), 1.2 (*2*), and 1.4 (*3*) TeV.

ton mass m_Y. The order of magnitude of the new contributions is proportional to t_θ, which means that these contributions must be much smaller than the standard contributions.

7. CONCLUSIONS

We have presented the economical 3–3–1 model with two-Higgs triplets. The minimal Higgs potential is considered in detail, with the prediction of a new Higgs bosons with the mass proportional to the bilepton mass. In the effective approximation, the charged Higgs bosons $H_2^\pm$ are scalar bileptons, while the neutral scalar bosons H_0 and H_1^0 do not carry a lepton number. The couplings of charged Higgs bosons to leptons and quarks are given. It follows that the Yukawa coupling of the charged Higgs boson to ordinary leptons and quarks are lepton-number violating. The pair production of $H_2^\pm$ at high-energy e^+e^- colliders with the polarization of the e^+, e^- beams was studied in detail. Numerical evaluation shows that, if the Higgs mass is not too large, then the production cross section may give observable values at moderately high energies at a high degree of polarization. We have also evaluated the associated production of $H_2^\pm$ and $W^\mp$ at high-energy e^+e^- colliders. It follows that the production cross sections are very small, much below the cross section of the pair production of $H_2^\pm$, and, therefore, the associated production of

$H_2^{\pm}$ and $W^{\mp}$ is, in general, not expected to lead to easily observable signals in e^+e^- annihilation. This is because the considered process is lepton-number violating ($\Delta L = \pm 2$).

Finally, we emphasize that the associated production of the charged Higgs boson and $W^{\mp}$ at high-energy e^+e^- colliders in the minimal supersymmetric SM was recently studied in [23]. However, this reaction first arises at the one-loop level, while the considered process in the economical 3–3–1 model exists at the tree level.

APPENDIX

Mixing Matrix of Neutral Gauge Bosons

For convenience in practical calculations, we use the mixing matrix

$$\begin{pmatrix} W_3 \\ W_8 \\ B \\ W_4 \end{pmatrix} = U \begin{pmatrix} A \\ Z^1 \\ Z^2 \\ W'_4 \end{pmatrix}, \qquad (A.1)$$

where

$$U = \begin{pmatrix} s_W & c_\varphi c_{\theta'} c_W & s_\varphi c_{\theta'} c_W & s_{\theta'} c_W \\ -\dfrac{s_W}{\sqrt{3}} & \dfrac{c_\varphi(s_W^2 - 3c_W^2 s_{\theta'}^2) - s_\varphi R_1 R_2}{\sqrt{3} c_W c_{\theta'}} & \dfrac{s_\varphi(s_W^2 - 3c_W^2 s_{\theta'}^2) + s_\varphi R_1 R_2}{\sqrt{3} c_W c_{\theta'}} & \sqrt{3} s_{\theta'} c_W \\ \dfrac{R_2}{\sqrt{3}} & -\dfrac{t_W(c_\varphi R_2 + s_\varphi R_1)}{\sqrt{3} c_{\theta'}} & -\dfrac{t_W(s_\varphi R_2 - c_\varphi R_1)}{\sqrt{3} c_{\theta'}} & 0 \\ 0 & -t_{\theta'}(c_\varphi R_1 - s_\varphi R_2) & -t_{\theta'}(s_\varphi R_1 + c_\varphi R_2) & R_1 \end{pmatrix},$$

$$R_1 = \sqrt{1 - 4s_{\theta'}^2 c_W^2}, \quad R_2 = \sqrt{4c_W^2 - 1},$$

and set

$$s_{\theta'} = \frac{t_{2\theta}}{c_W\sqrt{1 + 4t_{2\theta}^2}}.$$

In the approximation that we consider, the angle φ has to be very small [4]:

$$t_{2\varphi} \approx -\frac{\sqrt{3 - 4s_W^2}[v^2 + (11 - 14s_W^2)u^2]}{2c_W^4\omega^2}. \qquad (A.2)$$

ACKNOWLEDGMENTS

One of the authors (D.V.S.) expresses his sincere gratitude to the European Organization for Nuclear Research (CERN) for financial support. He is also grateful to J. Ellis for the hospitality during his visit at CERN, where this work was completed. This work was supported in part by the National Council for the Natural Sciences of Vietnam.

REFERENCES

1. Y. Fukuda et al. (Super-Kamiokande Collab.), Phys. Rev. Lett. **81**, 1562 (1998); **82**, 2644 (1999); **85**, 3999 (2000); **86**, 5651 (2001); Y. Suzuki, Nucl. Phys. B (Proc. Suppl.) **77**, 35 (1999); Y. Fukuda et al. (Super-Kamiokande Collab.), Phys. Rev. Lett. **81**, 1158 (1998); **82**, 1810 (1999); **86**, 5651 (2001).
2. F. Pisano and V. Pleitez, Phys. Rev. D **46**, 410 (1992); P. H. Frampton, Phys. Rev. Lett. **69**, 2889 (1992); R. Foot, O. F. Hernandez, F. Pisano, and V. Pleitez, Phys. Rev. D **47**, 4158 (1993).
3. R. Foot, H. N. Long, and Tuan A. Tran, Phys. Rev. D **50**, R34 (1994); J. C. Montero, F. Pisano, and V. Pleitez, Phys. Rev. D **47**, 2918 (1993); H. N. Long, Phys. Rev. D **54**, 4691 (1996); **53**, 437 (1996).
4. P. V. Dong, H. N. Long, D. T. Nhung, and D. V. Soa, Phys. Rev. D **73**, 035004 (2006).
5. J. J. F. Gunion, H. E. Haber, G. L. Kane, and S. Dawson, *The Higgs Hunter's Guide* (Addison-Wesley, Redwood City, Calif., 1990).
6. V. A. Ilyin, A. E. Pukhov, Y. Kurihara, et al., Phys. Rev. D **54**, 6717 (1996); A. Djouadi, H. E. Haber, and P. M. Zerwas, Phys. Lett. B **375**, 203 (1996); F. Boudjema and E. Chopin, Z. Phys. C **73**, 85 (1996).
7. S. Dawson, A. Dittmaier, and M. Spira, Phys. Rev. D **58**, 115012 (1998).
8. C. A. Baez, A. Gutierrez-Rodriguez, M. A. Hernandez-Ruiz, and O. A. Sampayo, Acta Phys. Slov. **56**, 455 (2006); Chong-Xing Yue, Lei Wang, and Li-Na Wang, Chin. Phys. Lett. **23**, 2379 (2006); P. Garcia-Abia, W. Lohmann, and A. R. Raspereza, Eur. Phys. J. C **44**, 481 (2005).
9. E. Accomando et al. (ECFA/DESY LC Physics Working Group Collab.), Phys. Rep. **299**, 1 (1998).
10. G. Jikia, Nucl. Phys. B **412**, 57 (1994).
11. P. V. Dong, H. N. Long, and D. V. Soa, Phys. Rev. D **73**, 075005 (2006).
12. H. N. Long and D. V. Soa, Nucl. Phys. B **601**, 361 (2001).
13. D. V. Soa, Takeo Inami, and H. N. Long, Eur. Phys. J. C **34**, 285 (2004).

14. D. V. Soa, H. N. Long, D. T. Binh, and D. P. Khoi, Zh. Éksp. Teor. Fiz. **125**, 755 (2004) [JETP **98**, 661 (2004)].
15. S. Godfrey, P. Kalyniak, and N. Romanenko, Phys. Lett. B **545**, 361 (2002).
16. J. E. Cienza Montalvo and M. D. Tonasse, Phys. Rev. D **71**, 095015 (2005).
17. L. D. Ninh and H. N. Long, Phys. Rev. D **72**, 075004 (2005).
18. W. Kilian, D. Rainwater, and J. Reuter, Phys. Rev. D **74**, 095003 (2006).
19. H. N. Long, Mod. Phys. Lett. A **13**, 1865 (1998); D. Chang and H. N. Long, Phys. Rev. D **73**, 053006 (2006).
20. W. A. Ponce, Y. Giraldo, and L. A. Sanchez, Phys. Rev. D **67**, 075001 (2003).
21. J. C. Montero, C. A. de S. Pires, and V. Pleitez, Phys. Rev. D **64**, 096001 (2001).
22. A. G. Dias, A. Doff, C. A. de S. Pires, and P. S. Rodrigues da Silva, Phys. Rev. D **72**, 035006 (2005).
23. H. E. Logan and S. Su, Phys. Rev. D **66**, 035001 (2002).